Molecular mechanisms of apoptosis promotion and inhibition of proliferation and metastasis through protein phosphatase 2A activation by *Zanthoxylum avicennae* extracts in HA22T hepatocarcinoma cells *in vitro* and *in vivo*

Tran Duc Dung[1,3], Wei-Wen Kuo[2], Truong Viet Binh[3], Chih-Yang Huang[1*]

[1]School of Chinese Medicine, China Medical University, Taichung, Taiwan
[2]Department of Biological Science and Technology, China Medical University, Taichung, Taiwan
[3]School of Chinese Medicine, Viet Nam Academy of Traditional Medicine, Ha Noi, Viet Nam

2012年傳統中藥與環境壓力調適國際研討會
International Conference of Traditional Chinese Medicine and Adaptation to Environmental Stress

Abstract

The use of herbs as alternative cancer therapies has attracted a great deal of attention owing to their lower toxicity. Whether *Zanthoxylum avicennae* (Ying Bu Bo, YBB) induces liver cancer cell apoptosis, inhibit proliferation and metastasis remains unclear. In this study, we investigated the effect of YBB extracts (YBBEs) on HA22T human hepatocellular carcinoma cells *in vitro* and in an *in vivo* mouse xenograft model. HA22T cells were treated with different concentrations of YBBEs and analyzed with MTT assay, flow cytometry, Western blot analysis, TUNEL, JC-1 staining, co-immuno-precipitation assay, RT-PCR and siRNA transfection assays. Additionally, the HA22T-implanted xenograft nude mice model was applied to confirm the cellular effects. YBBEs showed a strong inhibition of HA22T cell viability in a dose dependent manner and significantly reduced the cell proliferative proteins as well as induced cell cycle arrest in G2/M phase. YBBEs-induced apoptosis, up-regulated death receptor apoptotic pathway markers as well as mitochondrial proteins, and suppressed the survival proteins in a dose-dependent manner. Pro-survival Bcl-2 family proteins were inhibited and the pro-apoptotic ones were increased. YBBEs also demonstrated a high level of suppression of HA22T cell proliferation by cell migration inhibition by Boden chamber migration and invasion assays. When HA22T cells were treated with YBBEs, the cell migration-promoting proteins, uPA, tPA, MMP-2/-9, β-cartenin, p-GSK-3 β, TBX-3, and IL8 were downregated, however the migration-inhibiting proteins, PAI-1, TIMP-1/-2, GSK-3 β, APC and β-TrCP/HOS were significantly upregated. The expression of MMP-2/-9 and TIMP-1/-2 was assessed using RT-PCR and zymography assay, respectively. The mRNA levels and enzymatic activity of MMP-2/-9 were down-regulated by YBBEs treatment in a dose-dependent manner, while TIMP-1/-2 levels conversely markedly increased. It was also discovered that there was a decrease of the amount of β-catenin in the nucleus, meaning a significant nuclear export of that protein. In addition, PP2A siRNA or PP2A inhibitor totally blocked the YBBEs cell proliferation, metastasis inhibition and induced HA22T apoptosis. Finally, in the HA22T-implanted nude mice model, it was further confirmed that YBBEs inhibited tumor cell proliferation, metastasis and increased tumor cell apoptosis *in vivo*. All these results suggest that YBBEs is a potential candidate to inhibit HA22T hepatocellular carcinoma cell proliferation, metastasis and promote apoptosis *via* PP2A *in vitro* and *vivo*. In the near future, we would like to further investigate the YBBEs anticancer effect by preclinical studies and clinical trials.

Result

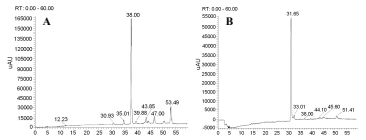

Figure 1. HPLC chromatographic profile of (A) YBBEs and (B) diosmin.

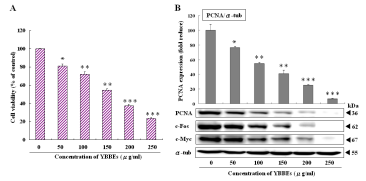

Figure 2. The suppressive effects of YBBEs on HA22T cell proliferation.
HA22T cells were incubated with 0, 50, 100, 150, 200 or 250 μg/ml of YBBEs for 24 h. (A) Cell viability as measured using MTT assay. (B) Downregulation of PCNA, c-Fos, and c-Myc proteins expression as revealed by western blot analysis; α-tubulin was used as a loading control. Data are shown as the means ± SE of three independent experiments and denote significant differences from control values with $^*p< 0.05$, $^{**}p< 0.01$ and $^{***}p< 0.001$, respectively.

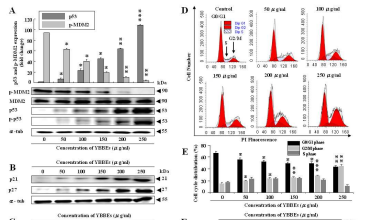

Figure 3. Cell cycle progression inhibition by YBBEs in hepatocellular carcinoma HA22T cells.
(A) Western blot analysis showing decreased p-MDM2 and increased p53 and p-p53 protein expression. (B and C) Cell cycle controlling protein expression was measured using western blot analysis with antibodies against the proteins indicated. Equal loading was assessed with an anti-α-tubulin antibody. (D) The cell cycle was determined using flow cytometric analysis. (E) Representative histograms clearly showing a significant YBBEs effect on inducing G2 phase cell cycle arrest in HA22T cells. (F) Western blot analysis showing decreased Cdc25C, Cdk1, and increased p-Cdc25C and p-Cdk1 protein expression.

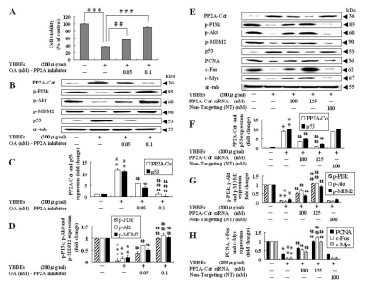

Figure 4. YBBEs inhibit HA22T cell viability through PP2A activation.
(A) The cell viability was examined using the MTT assay. (B) OA inhibits the YBBEs-induced inhibition of cell cycle progression by modulating the expression of PP2A-C α, p-PI3K, p-Akt, p-MDM2 and p53 proteins in HA22T cells. (E) siRNA knockdown of PP2A-C α to inhibit the YBBEs-induced inhibition of HA22T cell proliferation as determined by western blot analysis. α-tubulin was used as a loading control. (C and F) Bars represent the relative quantification of PP2A-C α and p53 relative to the control levels. (D and G) Bars represent the relative quantification of p-PI3k, p-Akt and p-MDM2 relative to the control levels. (H) Bars represent the relative quantification of PCNA, c-Fos and c-Myc relative to the control levels.

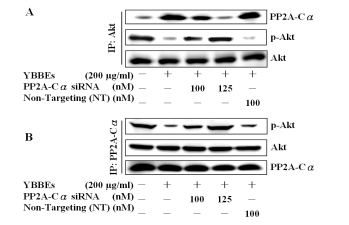

Figure 5. YBBEs-activated PP2A dephosphorylates phospho-Akt.
(A) Co-immunoprecipitation result regarding the degree of association of Akt with PP2A-C α, or p-Akt. (B) Co-immunoprecipitation result regarding the degree of association of PP2A-C α with p-Akt or Akt.

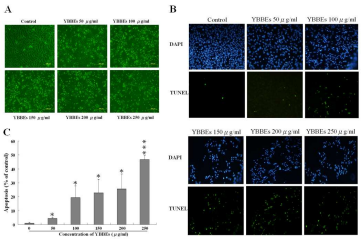

Figure 6. YBBEs induce apoptosis in human HA22T liver cancer cells.
(A) The morphological changes of viable HA22T cells after treatment with YBBEs. Photographs were taken on the morphological changes of HA22T cells and then observed under an inverted light microscope. (B) DAPI was used to label nuclei (upper panels) and apoptotic cell nuclei were labeled by TUNEL stain (lower panels). (C) Partition of positive apoptotic cells was based on percentages calculated from three sections of each treatment as described in Materials and methods.

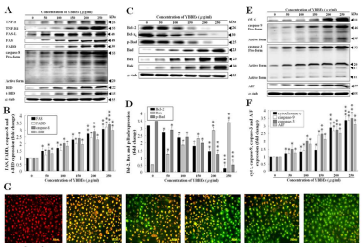

Figure 7. Effects of YBBEs on death receptor-dependent and mitochondria-dependent apoptotic pathways in the human hepatoma cell line, HA22T.
(A) TNF α, TNF-R1, FAS-L, FAS, FADD, caspase-8, BID and t-BID levels were examined by Western blot analysis. (C) Regulation of the Bcl-2 family proteins by YBBEs. (E) The protein expression levels of cytochrome c (cyt c), caspase-9, caspase-3 and apoptosis inducing factor (AIF) were measured by Western blotting. (G) The effects of YBBEs mitochondrial outer membrane permeability of HA22T cells.

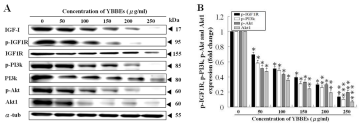

Figure 8. YBBEs supressed the IGF-I cell survival pathway.
(A) The protein expression levels (IGF-I, p-IGF1R, IGF1R, p-PI3k, PI3k, p-Akt and Akt) were measured by Western blotting. (B) Bars represent the relative quantification of p-IGF1R, p-PI3k, p-Akt and Akt1 on the basis of control level.

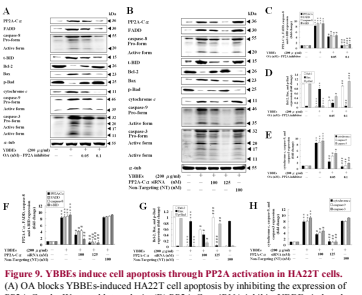

Figure 9. YBBEs induce cell apoptosis through PP2A activation in HA22T cells.
(A) OA blocks YBBEs-induced HA22T cell apoptosis by inhibiting the expression of PP2A-C α by Western blot analysis. (B) PP2A-C α siRNA inhibits YBBEs-induced HA22T cell apoptosis by Western blot analysis.

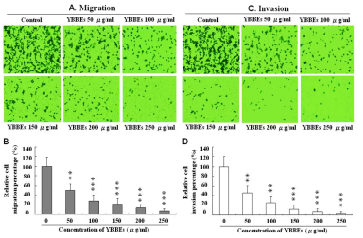

Figure 10. YBBEs effects on the HA22T cell migration and invasion *in vitro*.
(A) YBBEs effects on HA22T cell migration. (B) Quantitative cell number in migration assay. (C) YBBEs effects on HA22T cell invasion. (D) Quantitative cell number in invasion assay was done by counting at x200 and then observed under an inverted light microscope.

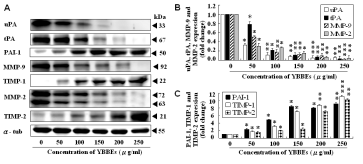

Figure 11. Suppressive effects of YBBEs on metastasis related proteins of HA22T cell.

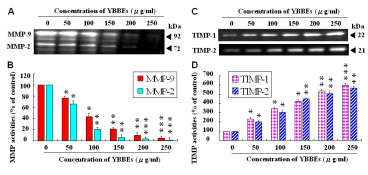

Figure 12. MMP-2/-9 and TIMP-1/-2 expression level activities were measured using gelatin zymography in HA22T cells.
(A) MMP-2/-9 protein expression was analyzed by gelatin zymography, which was performed on media conditioned by $2x10^5$ HA22T cells treated with YBBEs for 24 h. (B) The MMP-2 and MMP-9 enzyme activities in the treated cells were expressed as percentages of their activities in untreated cells. (C) TIMP-1/-2 protein expression was analyzed by gelatin zymography. (D) The TIMP-1 and TIMP-2 enzyme activities in the treated cells were expressed as percentages of their activities in untreated cells.

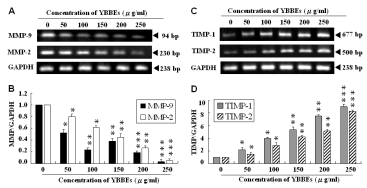

Figure 13. MMP-2/-9 and TIMP-1/-2 mRNA expression in HA22T cells as determined by RT-PCR analysis after the cells were treated with YBBEs.
The experiment was repeated three times with similar results. (A) MMP-2/-9 photograph of PCR products electrophoresis gel. (B) The MMP-2/GAPDH and MMP-9/GAPDH ratios in the cells treated with YBBEs at different concentrations were determined by densitometry. (C) TIMP-1/-2 photograph of an electrophoresis gel of PCR products. (D) The TIMP-1/GAPDH and TIMP-2/GAPDH ratios in the cells treated with YBBEs at different concentrations were determined by densitometry.

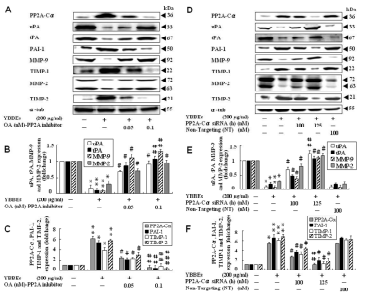

Figure 14. YBBEs inhibits HA22T cell migration and invasion effects through PP2A activation.

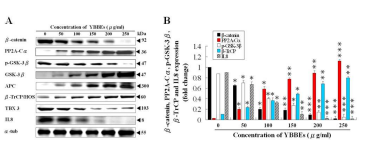

Figure 15. Inhibition of the metastatic function of beta-catenin by the treatment of YBBEs extraction in HA22T hepatocarcinoma cell line.

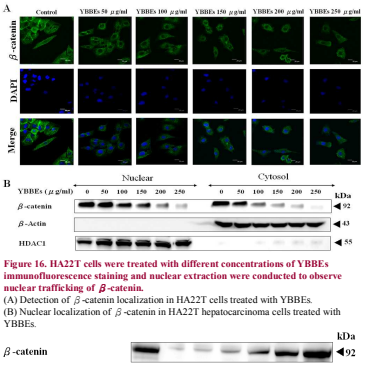

Figure 16. HA22T cells were treated with different concentrations of YBBEs immunofluorescence staining and nuclear extraction were conducted to observe nuclear trafficking of β-catenin.
(A) Detection of β-catenin localization in HA22T cells treated with YBBEs. (B) Nuclear localization of β-catenin in HA22T hepatocarcinoma cells treated with YBBEs.

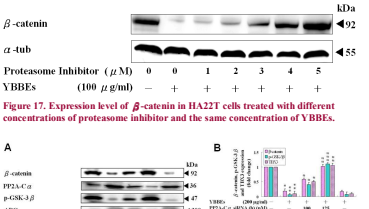

Figure 17. Expression level of β-catenin in HA22T cells treated with different concentrations of proteasome inhibitor and the same concentration of YBBEs.

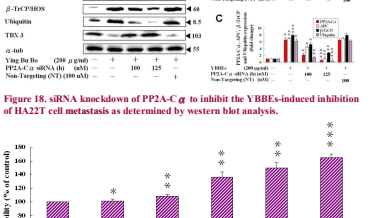

Figure 18. siRNA knockdown of PP2A-C α to inhibit the YBBEs-induced inhibition of HA22T cell metastasis as determined by western blot analysis.

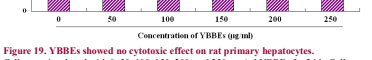

Figure 19. YBBEs showed no cytotoxic effect on rat primary hepatocytes.
Cells were incubated with 0, 50, 100, 150, 200, and 250 μg/ml YBBEs for 24 h. Cell viability was assessed by MTT assay.

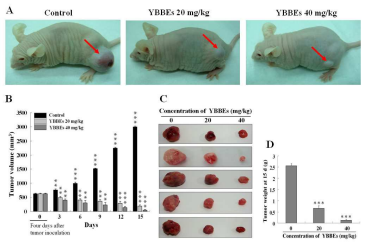

Figure 20. Effect of YBBEs on the growth of xenografted HA22T tumor tissue in nude mice.
HA22T cells ($1x10^6$ in 100 μl DMEM) were subcutaneously injected into the left flank of NU/NU mice. Starting at four days after inoculation, when the tumors had reached a volume around 600 mm^3, mice were orally treated with YBBEs (20 or 40 mg/kg) every day. (A) Representative pictures of drug-treated hepatomas. Red arrows indicate tumor mass. (B) Effect of YBBEs on final tumor volumes. (C) Photographic records of final harvested tumors. (D) Effect of YBBEs on final tumor weight.

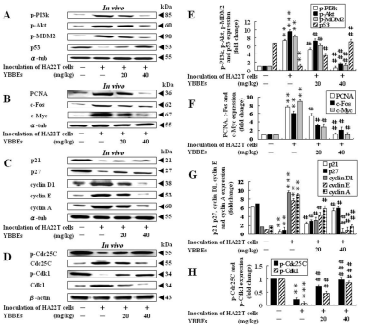

Figure 21. Western blot analysis in different tumor tissue groups in the HA22T xenograft nude mouse model treated or not treated with YBBEs.
(A-D) Western blot analysis of the expression levels of different proteins compared to the relative control values. (E) Bars representing the relative quantification of p-PI3k, p-Akt, p-MDM2 and p53 relative to the control levels. (F) Bars representing the relative quantification of PCNA, c-Fos and c-Myc relative to the control levels. (G) Bars representing the relative quantification of p21, p27, cyclin D1, cyclin E and cyclin A relative to the control levels. (H) Bars representing the relative quantification of p-Cdc25C and p-Cdk1 relative to the control levels.

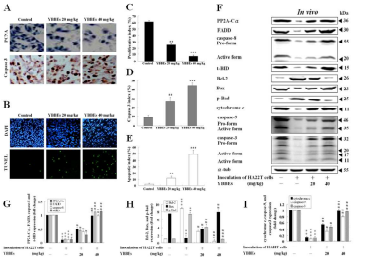

Figure 22. Immunohistochemistry studies and Western blot analysis of tumor tissues treated with different concentrations of YBBEs in HA22T xenograft nude mice model.
(A) Representative immunohistochemical stainings for PCNA and caspase-3. (B) Representative immunohistochemical stainings for TUNEL. (C) The proliferative and (D and E) apoptotic indices were calculated by the ratio of positive cells to total number of tumor cells counted. (F) Western blot analysis of the expression levels of different proteins compared to relative values of controls.

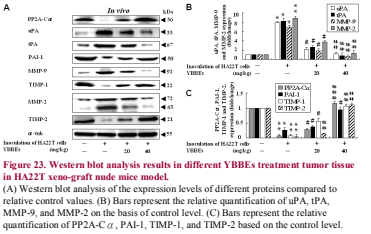

Figure 23. Western blot analysis results in different YBBEs treatment tumor tissue in HA22T xeno-graft nude mice model.
(A) Western blot analysis of the expression levels of different proteins compared to relative control values. (B) Bars represent the relative quantification of uPA, tPA, MMP-9, and MMP-2 on the basis of control level. (C) Bars represent the relative quantification of PP2A-C α, PAI-1, TIMP-1, and TIMP-2 based on the control level.

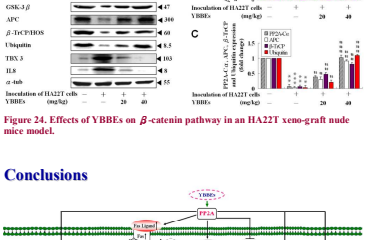

Figure 24. Effects of YBBEs on β-catenin pathway in an HA22T xeno-graft nude mice model.

Conclusions

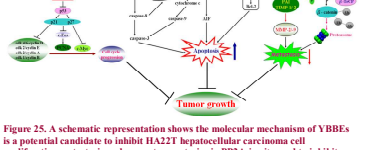

Figure 25. A schematic representation shows the molecular mechanism of YBBEs is a potential candidate to inhibit HA22T hepatocellular carcinoma cell proliferation,metastasis and promote apoptosis via PP2A *in vitro* and to inhibit xenografted HA22T tumor growth in the nude mice model.